Optimization of resonant effects in nanostructures via Weierstrass factorization

V. Grigoriev,[*] A. Tahri, S. Varault, B. Rolly, B. Stout, J. Wenger, and N. Bonod

Institut Fresnel (CNRS), Aix–Marseille Université, Campus St. Jérôme, Marseille 13013, France

Extensive numerical computations are often required to optimize the optical properties of nanostructures. Here, we use the Weierstrass factorization theorem to express the scattering matrix in terms of spectral singularities. We show that the location of poles and zeros of the scattering matrix fully determines all scattering properties, and that the scattering spectra of nanostructures can be decomposed into Lorentzian resonances over an arbitrary range of frequencies. This technique is applied to design nanoshell particles with enhanced absorption.

Resonant optical scatterers play a crucial role in nanoscale optics for concentrating and manipulating light far beyond the diffraction limit. To describe the scattering of light by nanoparticles, the Mie theory and its generalizations are often used as a theoretical framework [1]. However, the optimization of resonant properties requires extensive numerical computations which only provide a limited understanding of the underlying physics. A number of simplified models were introduced to bring more physical insight and to explain various resonant effects in nanostructures. Coupled oscillators and, more generally, coupled-mode theories [2,3] can be applied to describe Fano resonances [4–6], electromagnetically induced transparency and absorption [7–12], superscattering [13,14], as well as nonlinear effects [15–17]. Nevertheless, the coupled oscillator models are mostly used as a phenomenological tool which requires many fitting parameters and coupling factors [18–20].

Here, we propose an alternative approach based on the Weierstrass factorization theorem. We show that the singularities of the scattering matrix create a natural basis to decompose the scattering spectra of nanostructures. This approach determines all parameters of the coupled oscillators in a unique way and simplifies the optimization of resonant properties. As a typical example, we consider spherical nanoparticles and provide a detailed analysis of their spectra, including the optimization of absorption.

The scattering properties of any structure are fully characterized by the scattering matrix $S_l(\omega) = a_{\text{out}}/a_{\text{in}}$, which relates the amplitudes of outgoing a_{out} and ingoing a_{in} waves. It is assumed here that the S-matrix is diagonalized, which is always true for particles of spherical symmetry in the basis associated with electric and magnetic multipoles of a certain order l. Therefore, it is sufficient to consider the scattering process for each diagonal component, or scattering channel, separately.

The S-matrix is analytical anywhere in the complex frequency plane except for a discrete set of singular points. These singularities can be of two different types: poles and zeros. The frequencies ω_m^- at which the outgoing wave $a_{\text{out}} \neq 0$ can exist in the absence of external excitation $a_{\text{in}} = 0$ correspond to poles $S_l(\omega_m^-) \to \infty$. For passive structures without gain, the amplitude of such modes $a_{\text{out}}(t) = a_{\text{out}}(0)\exp(-i\omega_m^- t)$ should

decay as t increases due to the leakage of energy out of the structure. As a result, poles are always located in the lower part of the complex frequency plane $\text{Im}(\omega_m^-) < 0$. The frequencies ω_m^+ at which the ingoing wave $a_{\text{in}} \neq 0$ is fully absorbed $a_{\text{out}} = 0$ correspond to zeros $S_l(\omega_m^+) \to 0$. Usually, zeros are located in the upper part of the complex frequency plane $\text{Im}(\omega_m^+) > 0$.

The poles ω_m^- and zeros ω_m^+ of the S-matrix are related to perfectly emitting and absorbing modes of the system, because they satisfy the outgoing and ingoing boundary conditions, respectively. They can be considered as classical analogs of the creation and annihilation operators that are widely used in quantum mechanics. This formalism helps to build a consistent theory which describes the excitation of multiple resonances and the interplay among them [21].

In general, the knowledge of poles and zeros of some function is sufficient to restore it anywhere in the complex plane. This follows from the Weierstrass factorization theorem [22], which is often used in nuclear physics [23], but received surprisingly much less attention in electrodynamics and nanophotonics. Here, we apply it to decompose the S-matrix of spherical nanoparticles. The Weierstrass factorization for each diagonal component, or multipole l, takes the following form [24]:

$$S_l(\omega) = A \exp(iB\omega) \prod_m \frac{\omega - \omega_m^+}{\omega - \omega_m^-}, \qquad (1)$$

where A and B are constants defined as

$$A = S_l(0) \prod_m \frac{\omega_m^-}{\omega_m^+}, \qquad (2)$$

$$iB = \frac{S_l'(0)}{S_l(0)} + \sum_m \left(\frac{1}{\omega_m^+} - \frac{1}{\omega_m^-} \right). \qquad (3)$$

This factorization reexpresses the full S-matrix and all measurable quantities such as extinction or scattering cross sections in terms of singular points. From the physical point of view, the constants A and B are necessary to ensure a correct asymptotic behavior for infinitely long and short wavelengths. It is possible to prove that $S_l(0) = 1$ and $S_l'(0) = 0$ for structures of finite size [1], which further simplifies Eqs. (2) and (3).

The resonant frequencies $\omega_m^\pm$ can be found in a variety of different ways. If the function $S_l(\omega)$ can be computed for any complex frequency as in the Mie theory, then it is possible to extract the positions of zeros and poles by using root finding routines such as the Newton method [3]. A more general

---

*victor.grigoriev@fresnel.fr

approach which is suitable for the finite-element or boundary-element methods is to formulate an eigenvalue problem for the system and to solve it first with the outgoing boundary conditions and then with the ingoing ones. The two sets of the eigenvalues will correspond directly to the poles and zeros. Finally, it is possible to extract the resonant frequencies from experimental data by using a harmonic inversion technique either in time or in frequency domain [25,26].

Although the Weierstrass factorization is based on an infinite product, it can be readily converted to an infinite sum. The decomposition of Eq. (1) into partial fractions leads to the following formula [24]:

$$S_l(\omega) = A \exp(i B \omega) \left[1 + \sum_m \frac{\sigma_m}{\omega - \omega_m^-} \right], \qquad (4)$$

where σ_m are the residues which can be found as

$$\sigma_m = (\omega_m^- - \omega_m^+) \prod_{n \neq m} \frac{\omega_m^- - \omega_n^+}{\omega_m^- - \omega_n^-}. \qquad (5)$$

According to Eq. (4), each pole creates a peak of Lorentzian shape in the scattered spectra. The knowledge of the singularities $\omega_m^\pm$ fully determines not only the position $\mathrm{Re}(\omega_m^-)$ and half width $\mathrm{Im}(\omega_m^-)$ of these peaks, but also their strength σ_m so that there is no need to apply any fitting routine. A remarkable feature of Eq. (4) is that it predicts the presence of the term $\exp(i B \omega)$ which has been ignored in the models of coupled oscillators so far. This term accounts for retardation effects and becomes significant for structures whose size is comparable to the wavelength of light.

As an example, we apply our approach to a nanoshell structure [27]. The structure consists of a silica core with the radius 120 nm which is coated by a spherical gold layer with a thickness of 30 nm. The ambient medium is air with the refractive index $n(\omega) = 1$. To simplify the analysis, we take the refractive index of silica to be constant $n(\omega) = 1.45$. The permittivity of gold is described by the Drude formula $\varepsilon(\omega) = 1 - \omega_\mathrm{p}^2/(\omega^2 + i\Gamma\omega)$, where $\omega_\mathrm{p} = 7.28\omega_0$ and $\Gamma = 0.0215\omega_0$ [28]. All frequencies are specified in normalized units so that $\omega_0 = 2\pi c/\lambda_0$ corresponds to the wavelength $\lambda_0 = 1~\mu\mathrm{m}$ and the energy of photons $\hbar\omega_0 = 1.24$ eV. It is possible to use more accurate models for gold which take into account interband transitions [29–31] and to apply the empirical Sellmeier equation for the refractive index of silica [32]. However, the aim of this study is to demonstrate how the Weierstrass factorization helps to analyze the resonant properties of nanostructures. More sophisticated dispersion relations would simply lead to a larger number of poles and zeros in a given spectral range.

In the following, we consider the scattering channel of the S-matrix which corresponds to electric dipoles. All electric and magnetic multipoles of higher orders can be treated in a similar way. Figure 1 shows the map of the S_1 component in the complex frequency plane. The function $S_1(\omega)$ for this map was computed with the Mie theory [1]. Several singular points (poles ω_m^- and zeros ω_m^+) are clearly visible. The phase around them rotates by 2π in clockwise (poles) and counterclockwise (zeros) direction, which further confirms that these singularities are of the first order, or simple. Moreover,
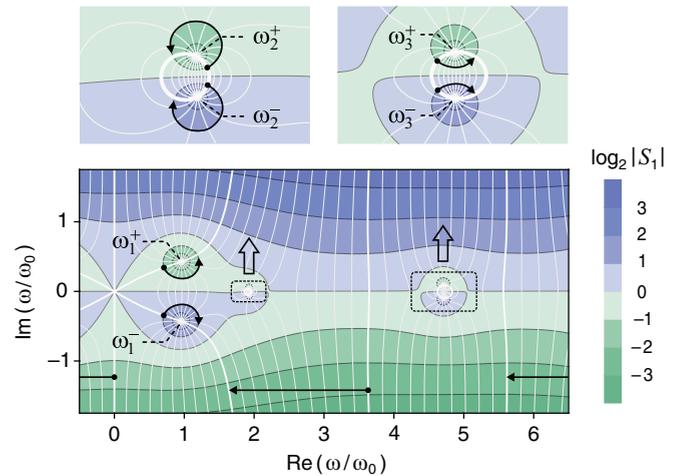

FIG. 1. (Color online) Map of the S_1 component (electric dipole) in the complex frequency plane for a spherical nanoparticle. The nanoparticle consists of a silica core (radius 120 nm) covered by a layer of gold (thickness 30 nm). The contours of blue and green shades show the absolute value of S_1 in a logarithmic scale. The positions of poles ω_m^- and zeros ω_m^+ are labeled on the plot. The regions of the plot which are inside dashed rectangles are magnified in the insets on the top. The white contour lines show the phase of S_1 in the steps of π for thick lines and $\pi/10$ for thin lines. The black arrows indicate the direction in which the phase grows from 0 to π.

since the components of the S-matrix are single-value functions, there is no need to introduce any branch cuts.
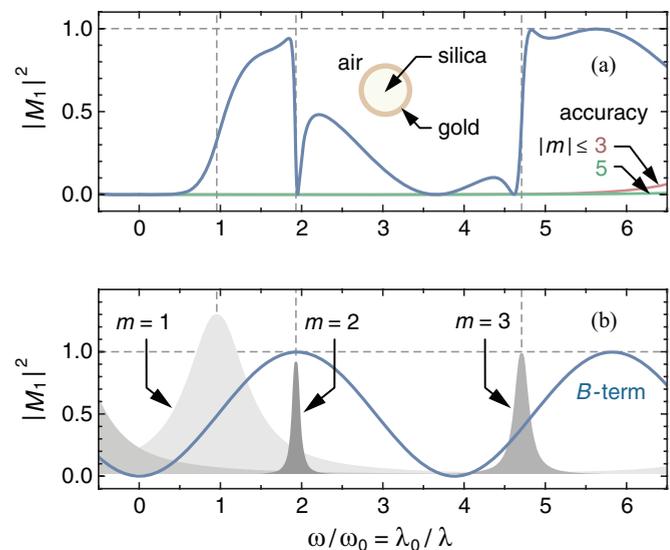

FIG. 2. (Color online) (a) The Mie coefficient M_1 (electric dipole) as a function of frequency for the nanoparticle with the same parameters as in Fig. 1. The spectrum can be computed with the Mie theory (blue line) or as a sum of Lorentzian resonances according to Eq. (4). The difference between these representations (red and green lines) vanishes if a sufficiently large number of resonances is taken into account. The positions of these resonances are indicated by vertical dashed lines. (b) The contribution of various terms to the Mie coefficient: Lorentzian resonances (gray contours) and a retardation term (blue line).
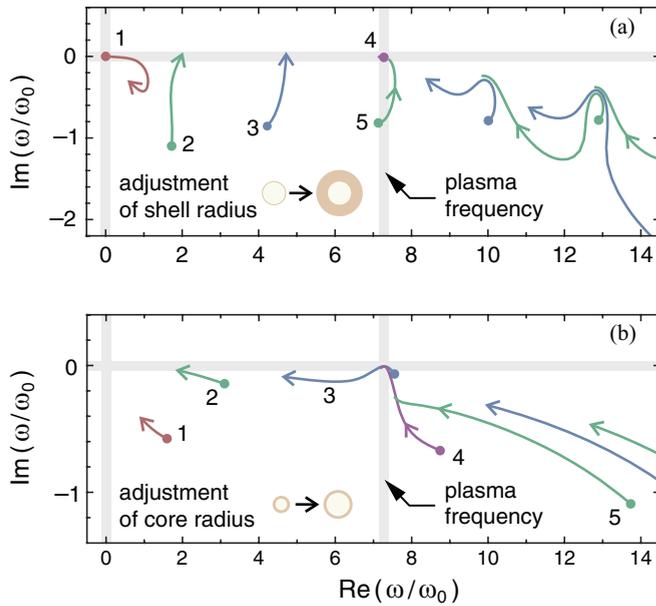
FIG. 3. (Color online) The movement of the poles ω_m^- in the complex frequency plane as the radius of the layers in the nanoshell structure is adjusted. (a) The radius of the core is fixed to 120 nm, while the thickness of the shell is varied from 0 to 120 nm. Notice that the path of the poles is different before and after the plasma frequency (vertical gray line). (b) The radius of the core is varied from 60 to 120 nm, while the thickness of the shell is set to 30 nm. The numbering of the poles is consistent with Fig. 2.

The positions of poles and zeros satisfy some symmetry relations which can be derived from the general properties of the S-matrix. Since the response to an excitation described by a real function must be a real function [23], the following relation holds: $[S_l(\omega)]^* = S_l(-\omega^*)$. As a result, the singularities always exist in pairs $\{\omega_m^\pm, -(\omega_m^\pm)^*\}$ which are mirror symmetric with respect to the imaginary axis. If the structure is lossless, the S-matrix is unitary $|S_l(\omega)|^2 = 1$ for all real frequencies [23], because the out- and ingoing waves carry the same amount of energy. As a consequence, the poles and zeros are not independent and can be related to each other, $\omega_m^+ = (\omega_m^-)^*$. This property remains approximately valid for lossy structures which contain metals as shown in Fig. 1.

Many other spectra such as Mie coefficients or effective polarizabilities can be expressed in terms of the S-matrix. For example, the Mie coefficients M_l can be computed as $M_l = (S_l - 1)/2$, and Fig. 2 shows the spectrum of the M_1 coefficient (electric dipole) together with its decomposition into Lorentzian peaks. The B term creates a nonzero background $|[A \exp(iB\omega) - 1]/2|^2$ for the peaks, and it can be written approximately as $[1 - \cos(B\omega)]/2$ if $A \approx 1$. The superpositions of Lorentzian peaks with each other and with the background term produce asymmetric Fano shapes [33]. They are particulary pronounced around the frequencies $1.9\omega_0$ and $4.7\omega_0$ in Fig. 2(a).

The Lorentzian decomposition is based on the formulas (4) and (5) which are valid for an arbitrary number of resonances. In general, it can be problematic to find all of them because even the simplest optical structures such as

dielectric multilayers have an infinite number of resonances [34]. However, the optical structures are usually studied in a limited range of frequencies, and r is sufficient to take into account only those resonances which can be excited by the sources in the infrared or visible range. Figure 2(a) is very illustrative in this regard, since it shows that three pairs of poles and zeros provide a remarkably good accuracy over a broad range of frequencies. The width of the range is only limited by the presence of other resonances at higher frequencies. By including more and more resonances into the Weierstrass factorization, the range of validity can be made arbitrarily wide.

It is worth noting that $M_l(\omega)$ and $S_l(\omega)$ have a common set of poles, but their zeros are different. The zeros of $M_l(\omega)$ appear at those points where $|S_l| = 1$ and $\arg(S_l) = 0$ (cf. Fig. 1). The same conclusions can be applied for the effective polarizability $\alpha(\omega)$ of the nanoparticle, because it is proportional to the Mie coefficient, $\alpha = (3M_1)/(2ik^3)$, where k is the wave number in the ambient medium [35]. The effective polarizabilities in the quasistatic limit can be computed very
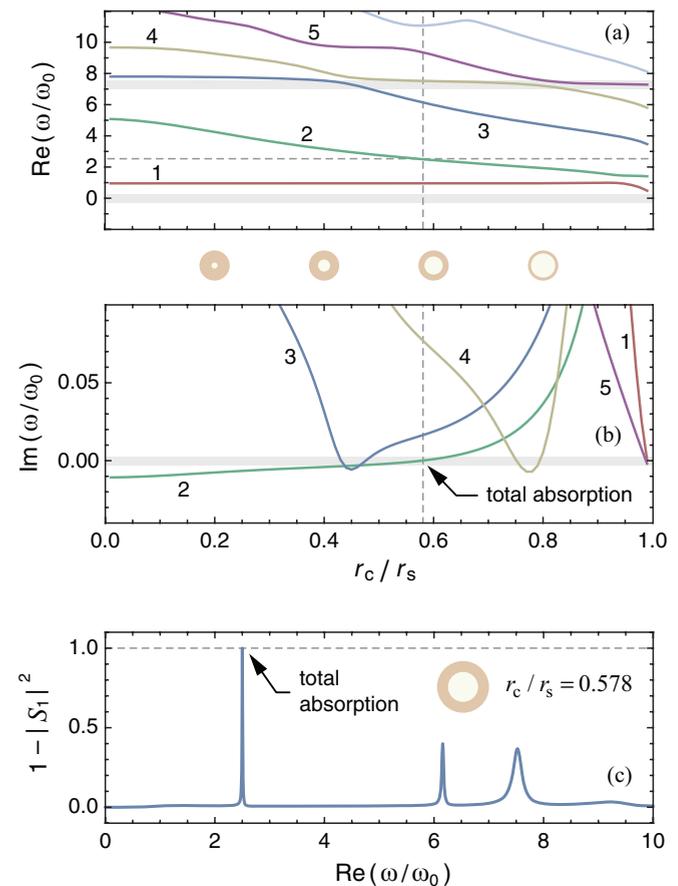

FIG. 4. (Color online) Optimization of absorption in the nanoshell structure. The real (a) and imaginary (b) parts of the zeros ω_m^+ are shown as a function of r_c/r_s, where r_c is the core radius, and r_s is the total size of the structure which is fixed to 150 nm. A schematic picture in the middle shows how the geometry of the structure changes during the optimization. Total absorption occurs if for some mode $\text{Im}(\omega_m^+) = 0$. This condition can be satisfied at $r_c/r_s = 0.578$, as indicated in the plot. (c) The absorption spectrum of the optimized nanoshell structure.

efficiently with the Weierstrass factorization. By noticing that $\alpha(0) = S_1'''(0)c^3/(8i)$ and substituting the third derivative of Eq. (1), one obtains the following formula,

$$\alpha(0) = \frac{c^3}{4i} \sum_m \left[\frac{1}{(\omega_m^-)^3} - \frac{1}{(\omega_m^+)^3} \right], \qquad (6)$$

which converges very rapidly due to the third power of the resonant frequencies. The effective polarizabilities of the nanoshell structures can be further used to compute the effective permittivity and permeability of composite media [36].

It is possible to control the positions of poles and zeros by varying the parameters of the structure. If the thickness of the metal shell is increased, the tunneling of waves through it is reduced, and the poles shift towards the real axis [Fig. 3(a)]. This is especially true for poles which are below plasma frequency ω_p. If the radius of the core is increased, the poles move to lower frequencies [Fig. 3(b)], because standing waves with the same number of peaks can fit into a larger structure at smaller frequencies.

The pole tracking diagrams are useful to explain the origin of the poles. When the thickness of the shell is infinitely small [Fig. 3(a)], it can still create a sufficiently strong reflection when either $\varepsilon(\omega) = \infty$ or $\varepsilon(\omega) = 0$. According to the Drude formula, this happens at the frequencies $\omega \approx 0$ and $\omega \approx \omega_p$. Therefore, the poles ω_1^- and ω_4^- can be identified with the singularities of the Drude model. All other poles tend to an equidistant distribution, which resembles the standing-wave modes of the Fabry-Pérot resonator.

Since zeros account for the absorption processes, following their trajectories in the complex plane allows us to optimize the absorption in nanoshell structures. While the trajectories of poles are restricted to the lower part of the complex frequency plane, zeros do not have such a limitation and can cross the

real axis $\mathrm{Im}(\omega_m^+) = 0$. This means that a total absorption can be observed at real frequencies. It often occurs in metallic gratings for plane waves incident at a certain angle [37,38], and it is interesting to see whether a similar effect happens for nanoshell structures.

Figure 4 shows the real and imaginary parts of the zeros when a scan over the parameters of the nanostructure is performed. One of the zeros (ω_2^+) crosses the real frequency axis when the ratio of core and shell radii is equal to 0.578. We selected this zero because it can be observed at the lowest frequency $\mathrm{Re}(\omega_m^+)$. The absorption spectrum for the optimized geometry is shown in Fig. 4(c), which confirms that a total absorption can be achieved in the scattering channel of electric dipoles. Such coherent absorbers can be considered as time-reversed lasers [39] and are promising for applications in nano-optics [40].

In conclusion, a semianalytical approach was developed to describe the resonant properties of nanostructures. It does not require any fitting parameters and relies on the Weierstrass factorization theorem to express all spectra in terms of singularities. This approach simplifies the design of resonant properties for applications, and as an example, it was shown how to optimize absorption in nanoshell structures. We believe that this formalism is not limited to single scatterers and can be readily extended to periodic structures such as diffraction gratings or metamaterials.

[1] C. F. Bohren and D. R. Huffman, *Absorption and Scattering of Light by Small Particles* (Wiley, New York, 1983).

[2] H. A. Haus, *Waves and Fields in Optoelectronics* (Prentice-Hall, Englewood Cliffs, NJ, 1984).

[3] C. E. Baum, in *Transient Electromagnetic Fields*, edited by L. Felsen, Topics in Applied Physics Vol. 10 (Springer, Berlin, 1976), pp. 129–179.

[4] S. Fan, W. Suh, and J. D. Joannopoulos, J. Opt. Soc. Am. A **20**, 569 (2003).

[5] V. Giannini, Y. Francescato, H. Amrania, C. C. Phillips, and S. A. Maier, Nano Lett. **11**, 2835 (2011).

[6] B. Gallinet and O. J. F. Martin, Phys. Rev. B **83**, 235427 (2011).

[7] N. Liu, L. Langguth, T. Weiss, J. Kastel, M. Fleischhauer, T. Pfau, and H. Giessen, Nat. Mater. **8**, 758 (2009).

[8] R. Taubert, M. Hentschel, J. Kastel, and H. Giessen, Nano Lett. **12**, 1367 (2012).

[9] P. Tassin, L. Zhang, R. K. Zhao, A. Jain, T. Koschny, and C. M. Soukoulis, Phys. Rev. Lett. **109**, 187401 (2012).

[10] P. Tassin, L. Zhang, T. Koschny, E. N. Economou, and C. M. Soukoulis, Phys. Rev. Lett. **102**, 053901 (2009).

[11] M. F. Yanik, W. Suh, Z. Wang, and S. H. Fan, Phys. Rev. Lett. **93**, 233903 (2004).

[12] Q. F. Xu, S. Sandhu, M. L. Povinelli, J. Shakya, S. H. Fan, and M. Lipson, Phys. Rev. Lett. **96**, 123901 (2006).

[13] Z. Ruan and S. Fan, Phys. Rev. Lett. **105**, 013901 (2010).

[14] L. Verslegers, Z. Yu, Z. Ruan, P. B. Catrysse, and S. Fan, Phys. Rev. Lett. **108**, 083902 (2012).

[15] V. Grigoriev and F. Biancalana, Phys. Rev. A **83**, 043816 (2011).

[16] V. Grigoriev and F. Biancalana, Opt. Lett. **36**, 2131 (2011).

[17] M. F. Yanik, S. Fan, M. Soljacic, and J. D. Joannopoulos, Opt. Lett. **28**, 2506 (2003).

[18] B. Gallinet and O. J. F. Martin, ACS Nano **5**, 8999 (2011).

[19] Y. Francescato, V. Giannini, and S. A. Maier, ACS Nano **6**, 1830 (2012).

[20] S. Mukherjee, H. Sobhani, J. B. Lassiter, R. Bardhan, P. Nordlander, and N. J. Halas, Nano Lett. **10**, 2694 (2010).

[21] A. S. Davydov, *Quantum Mechanics*, 2nd ed. (Pergamon, Oxford, U.K., 1976).

[22] A. I. Markushevich, *Theory of Functions of a Complex Variable*, 2nd ed. (AMS, New York, 1977).

OPTIMIZATION OF RESONANT EFFECTS IN . . .   PHYSICAL REVIEW A **88**, 011803(R) (2013)

[23] R. G. Newton, *Scattering Theory of Waves and Particles*, 2nd ed. (Springer, New York, 1966).

[24] See Supplemental Material at http://link.aps.org/supplemental/10.1103/PhysRevA.88.011803 for an alternative proof of the Weierstrass factorization theorem in the case of functions which have poles and zeros of the first order.

[25] V. A. Mandelshtam, Prog. Nucl. Magn. Reson. Spectrosc. **38**, 159 (2001).

[26] B. Gustavsen and A. Semlyen, IEEE Trans. Power Delivery **14**, 1052 (1999).

[27] E. Prodan, C. Radloff, N. J. Halas, and P. Nordlander, Science **302**, 419 (2003).

[28] M. A. Ordal, R. J. Bell, J. R. W. Alexander, L. L. Long, and M. R. Querry, Appl. Opt. **24**, 4493 (1985).

[29] F. Hao and P. Nordlander, Chem. Phys. Lett. **446**, 115 (2007).

[30] A. Vial and T. Laroche, Appl. Phys. B **93**, 139 (2008).

[31] A. D. Rakic, A. B. Djurisic, J. M. Elazar, and M. L. Majewski, Appl. Opt. **37**, 5271 (1998).

[32] M. J. Weber, *Handbook of Optical Materials* (CRC, Boca Raton, FL, 2002).

[33] B. Luk'yanchuk, N. I. Zheludev, S. A. Maier, N. J. Halas, P. Nordlander, H. Giessen, and C. T. Chong, Nat. Mater. **9**, 707 (2010).

[34] V. Grigoriev and F. Biancalana, Opt. Lett. **36**, 3774 (2011).

[35] B. Stout, A. Devilez, B. Rolly, and N. Bonod, J. Opt. Soc. Am. B **28**, 1213 (2011).

[36] M. S. Wheeler, J. S. Aitchison, and M. Mojahedi, Phys. Rev. B **73**, 045105 (2006).

[37] M. C. Hutley and D. Maystre, Opt. Commun. **19**, 431 (1976).

[38] E. Popov, S. Enoch, and N. Bonod, Opt. Express **17**, 6770 (2009).

[39] Y. D. Chong, L. Ge, H. Cao, and A. D. Stone, Phys. Rev. Lett. **105**, 053901 (2010).

[40] A. Sentenac, P. C. Chaumet, and G. Leuchs, Opt. Lett. **38**, 818 (2013).